# 3.7 Testing the Radiosonde Replacement System (RRS) Radiosondes in a Maritime Polar Environment

Jim Fitzgibbon and Joe Facundo, NWS, Office of Operational Systems, and Nick Schmidt, QSS Group Inc., Sterling, Virginia

## 1. Introduction

NOAA's, National Weather Service (NWS) conditionally qualified the Sippican Mark IIA radiosonde for use in their upper air network. Over the course of evaluating the conditionally-qualified radiosonde, additional problems were identified. Sippican, in an effort to minimize the problems identified, implemented changes in their production process, their humidity duct design, and temperature boom positioning procedures. To ensure the radiosondes perform correctly over the range of weather conditions encountered at the NWS upper air sites, the NWS would normally conduct a test spanning at least three seasons. To expedite this process, the NWS selected four different field sites, each with different climatological characteristics. This paper covers the functional precision testing at only one of those sites selected (Quillayute, Washington).

Quillayute was selected to evaluate the radiosonde in the maritime polar air mass which usually dominates the weather over the coastal areas of the Pacific Northwest during the winter months. Conditions expected for the test were cool temperatures with overcast low clouds and rain.

## 2. Functional Precision Testing

Functional precision tests are conducted to determine the amount of measurement variability that exists between two identical instruments. For this test, the two instruments were simultaneously exposed to the same environment. To determine the functional precision, the root mean square of the differences (MSD) is calculated for each parameter. For this test the functional precision was determined for each of the meteorological sensors and the GPS u and v wind components.

## 3. Test Methodology

Each flight train consisted of an 800 or 1000 gram balloon, two parachutes, and a 6-foot Styrofoam spreader bar used for separating the two radiosondes from each other. The overall flight train length was 100 to 120 feet.

Figure 1 shows the flight train configuration for flying two radiosondes simultaneously. Radiosonde transmitter frequencies were selected so that separation in the 1680 MHz band is sufficient to eliminate frequency interference between the two radiosondes.

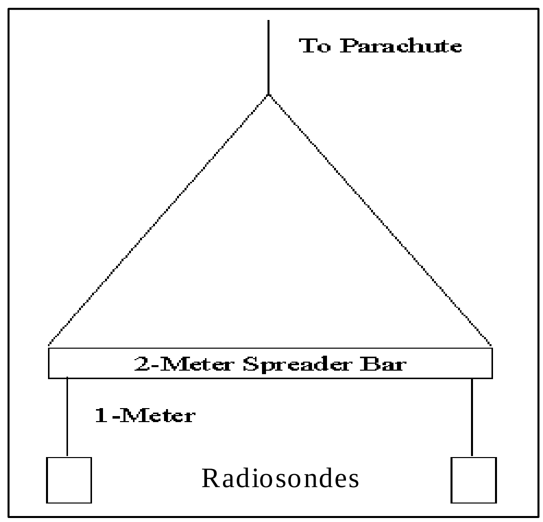


**Figure 1. Dual flight train assembly**

To have a good statistical sample, the NWS will usually conduct forty to fifty dual radiosonde flights for a functional precision test. For this portion of the test there were only 10 flights conducted. As such, the results are presented as a first look at these data and should only be used as an indicator of the overall functional precision of the radiosonde. Once testing is completed at all sites, data will be combined to have a more definitive answer of the functional precision.

## 4. Data Analysis

The radiosonde data was collected from the vendor supplied Signal Processing System (SPS) using the NWS-written program, "Protocol Interface Test Suite" (PITS). PITS files were then normalized into one-second intervals using an NWS utility called Convert PITS. Convert PITS is also used to calculate the geopotential height, apply the surface pressure discrepancy, and a newly adopted solar radiation correction scheme.

For this test, the data were analyzed on a flight-by-flight basis and as grouped flights to determine the functional precision of the radiosonde. The flight-by-flight data analysis was conducted for both the raw and corrected data sets. The statistical analysis was conducted using the corrected normalized one-second data set. This paper only covers the statistical analysis.

Once normalized using Convert PITS, the data were time-paired and entered into SPSS©[1] to calculate the differences and for the generation of statistics for each of the measured parameters. The corrected data sets were chosen for the statistical analysis because they were processed in nearly the same manner as will be fielded with the Radiosonde Replacement System (RRS).

### 4.1 Statistical Analysis of Pressure Data

For the entire flight series, 100% of the absolute pressure differences by time were equal to or less than 1.31 hPa and 95% were equal to or less than 0.54 hPa. Figure 2 depicts the cumulative percentages for the absolute value of the pressure differences, and figure 3 illustrates the distribution or the actual pressure differences. The interval size used for the histogram in Figure 3 was 0.4 hPa.

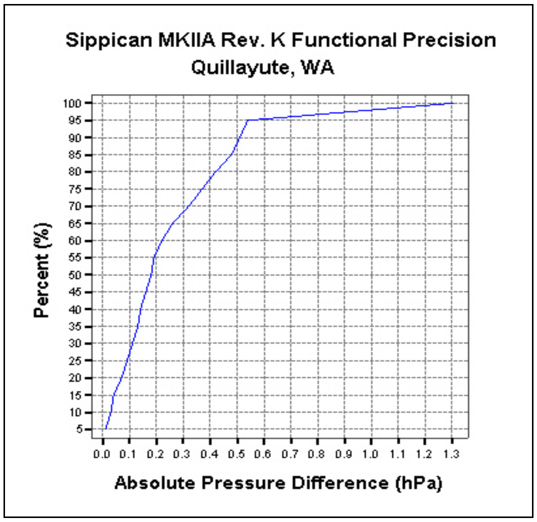


**Figure 2. Graph of Cumulative percentages of absolute pressure differences.**

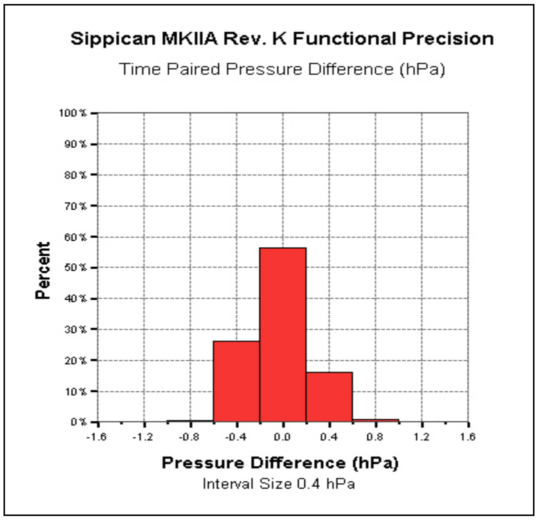


**Figure 3. Histogram of pressure difference.**

The scatter plot shown in Figure 4 indicates good agreement across the entire range of measurements, without any large outliers.

[1] SPSS is a statistical processing software package developed by SPSS Inc.

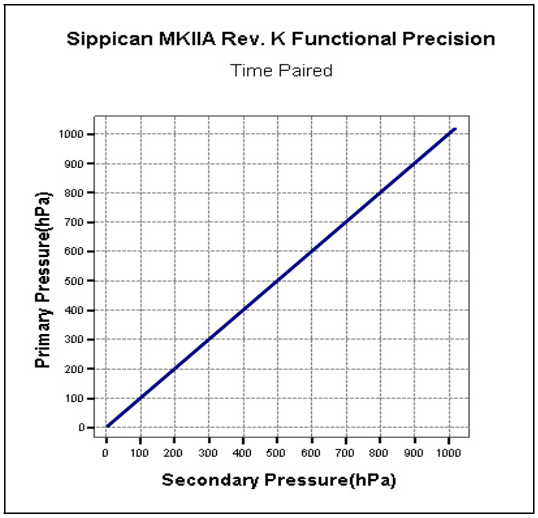


**Figure 4. Scatter plot of pressure values for all flights.**

For the ten flight series, the overall functional precision (RMSD) for the time-paired pressure measurements was 0.29 hPa and the mean of the differences was -0.03 hPa. A mean difference this small indicates there is no systematic bias induced by the ground equipment. Table 1 is the summary statistics for the entire test series and for specified intervals of pressure.

| Time Paired Pressure Difference Statistics | | | | | |
|---|---|---|---|---|---|
| Intervals (hPa) | N Sample | Min | Max | Mean | RMSD |
| **19.9 to 0** | 8773 | -0.57 | 0.63 | -0.07 | 0.30 |
| **49.9 to 20** | 10569 | -0.59 | 0.55 | -0.04 | 0.29 |
| **99.9 to 50** | 8541 | -0.58 | 0.48 | -0.03 | 0.27 |
| **199.9 to 100** | 8747 | -0.66 | 0.39 | -0.04 | 0.25 |
| **299.9 to 200** | 4675 | -0.8 | 0.52 | -0.06 | 0.28 |
| **499.9 to 300** | 6537 | -0.76 | 0.82 | -0.06 | 0.30 |
| **849.9 to 500** | 7934 | -0.85 | 0.97 | 0.01 | 0.31 |
| **1070 to 850** | 3018 | -0.78 | 1.31 | 0.12 | 0.35 |
| **ALL** | 58794 | -0.85 | 1.31 | -0.03 | 0.29 |
| **400 to 4** | 44881 | -0.8 | 0.63 | -0.05 | 0.28 |
| **SFC to 400** | 13913 | -0.85 | 1.31 | 0.02 | 0.32 |

**Table 1. Summary statistics for the time paired pressure differences.**

### 4.2 Statistical Analysis of Temperature Data

For the entire flight series, 99% of the absolute temperature differences by time were equal to or less than 0.81 ºC and 95% were equal to or less than 0.50 ºC. Figure 5 depicts the cumulative percentages for the absolute value of the temperature differences, and figure 6 illustrates the distribution or the actual temperature differences.

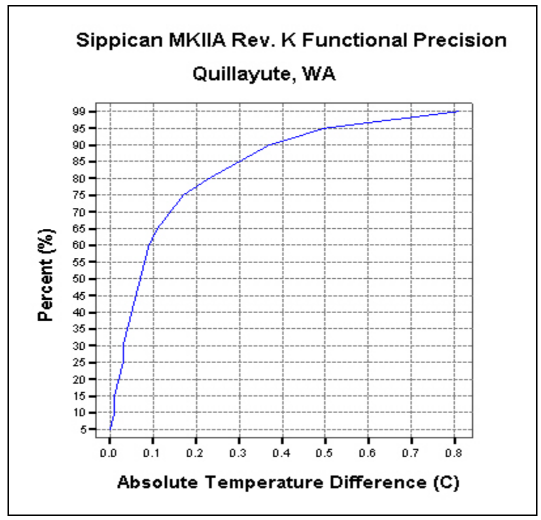


**Figure 5. Graph of Cumulative percentages of absolute temperature differences.**

The y-axis in figure 5 was scaled to 99 percent to maintain usefulness; large difference outliers in the last one percent compressed the x-axis and reduced usefulness. The interval size used for the histogram in figure 6 was 0.4 ºC.

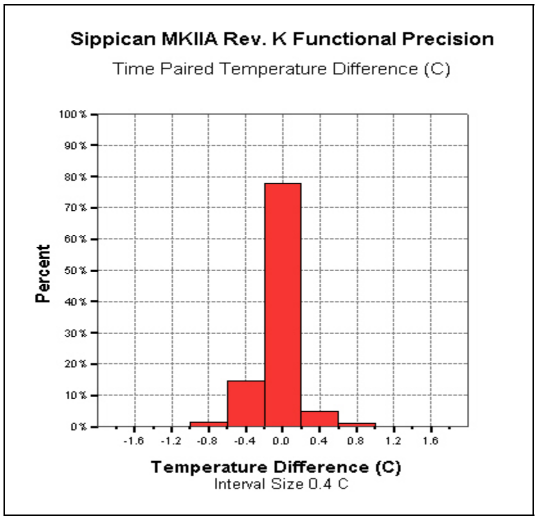


**Figure 6. Histogram of temperature differences.**

The scatter plot shown in Figure 7 indicates good temperature agreement for most of the temperature measurements. It has been suggested that the outliers between -20 and -10 ºC are associated with the latent heat released during a change in state from liquid to frozen. Figure 8 contains an example of a dual flight with a temperature spike that is perhaps related to a change in state. All known cases of spikes like this have occurred in stratums where there was a significant decrease in humidity and temperatures were between -10 to -30 ºC. Although it was difficult to see, this temperature spike occurred on both radiosondes at nearly the same time.

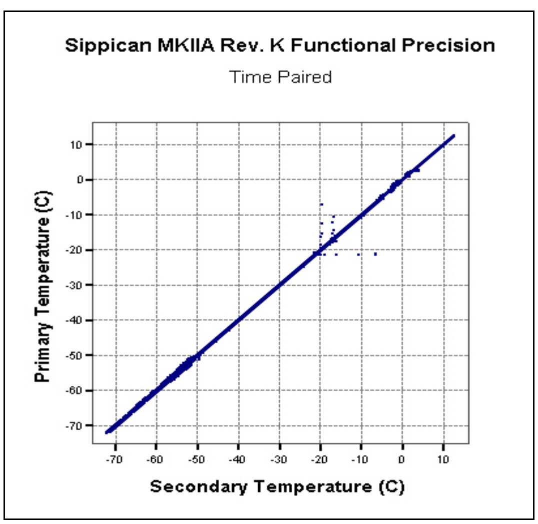


**Figure 7. Scatter plot of temperature values for all flights.**

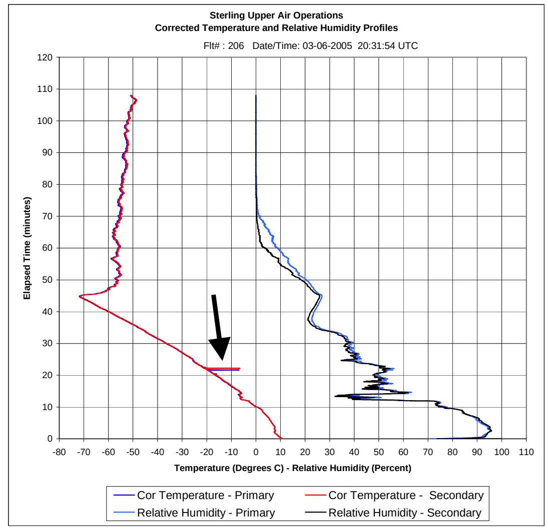


**Figure 8. Temperature profile with latent heat temperature spike.**

For the ten flight series, the overall functional precision (RMSD) for the time paired temperature measurements was 0.26 ºC and the mean of the differences was 0.05 ºC. A mean difference this small indicates there is no systematic bias induced by the ground equipment. Table 2 is the summary statistics for the entire test series and for specified intervals of temperature.

| Time Paired Temperature Difference Statistics | | | | | |
|---|---|---|---|---|---|
| **Intervals (hPa)** | **N Sample** | **Min** | **Max** | **Mean** | **RMSD** |
| **19.9 to 0** | 8773 | -1.11 | 1.3 | -0.12 | 0.36 |
| **49.9 to 20** | 10569 | -0.84 | 0.97 | -0.06 | 0.25 |
| **99.9 to 50** | 8541 | -1 | 0.89 | -0.03 | 0.21 |
| **199.9 to 100** | 8747 | -0.64 | 0.67 | -0.03 | 0.16 |
| **299.9 to 200** | 4675 | -0.46 | 0.58 | -0.03 | 0.13 |
| **499.9 to 300** | 6537 | -14.55 | 12.76 | -0.04 | 0.40 |
| **849.9 to 500** | 7934 | -1.53 | 6.39 | -0.01 | 0.21 |
| **1070 to 850** | 3018 | -0.52 | 0.26 | 0.00 | 0.04 |
| **ALL** | 58794 | -14.55 | 12.76 | -0.05 | 0.26 |
| **400 to 4** | 44881 | -1.11 | 1.3 | -0.06 | 0.24 |
| **SFC to 400** | 13913 | -14.55 | 12.76 | -0.02 | 0.31 |

**Table 2. Summary statistics for the time paired temperature differences.**

### 4.3 Statistical Analysis of Relative Humidity Data

For the entire flight series, the absolute relative humidity differences by time were equal to or less than 14.50% RH and 95% of the differences were equal to or less than 8.10%. Figure 9 depicts the cumulative percentages for the absolute value of the relative humidity differences, and figure 10 illustrates the distribution or the actual relative humidity differences.

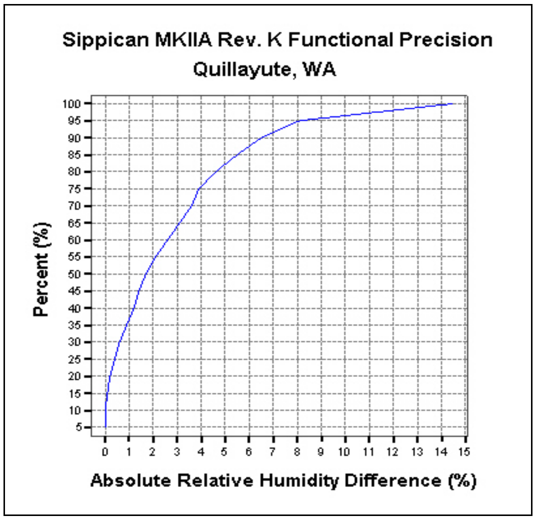


**Figure 9. Graph of cumulative percentages of absolute Relative Humidity differences.**

The interval size used for the histogram in figure 10 was 5%.

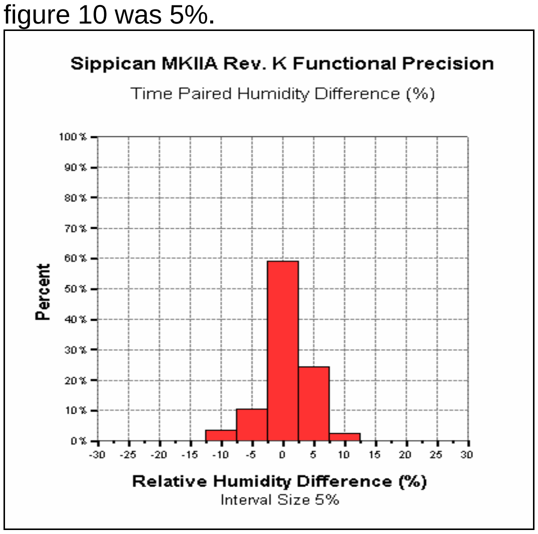


**Figure 10. Histogram of relative humidity difference.**

The scatter plot shown in Figure 11 indicates a divergence at low relative humidity; this is suspected to be associated with two different phenomena. The first is suspected to be a hysteresis issue that occurs when the instrument transitions from a very high to a very low humidity, usually occurring in the lower troposphere. The second is suspected to be associated with an inconsistent reduction in response times between the two radiosondes. This typically occurs at higher altitudes when temperatures are below -25 ºC.

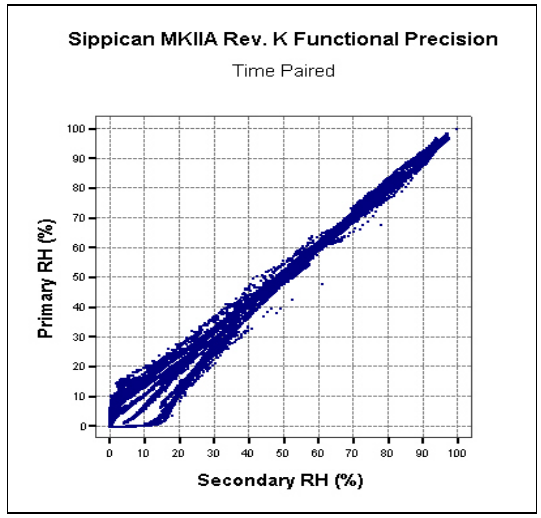


**Figure 11. Scatter plot of relative humidity values for all flights.**

Figure 12 is a temperature and humidity profile for one of the dual flights conducted. Point A is an example of the hysteresis which occurs after the radiosondes transition from a very high humidity to a very low humidity. Point B illustrates the latencies in the response time between the two radiosondes.

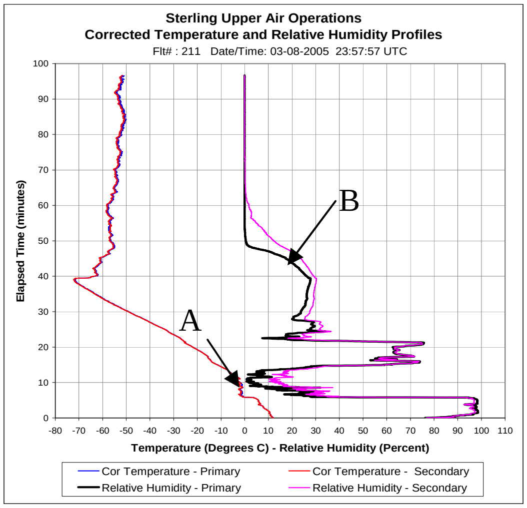


**Figure 12. Dual flight RH profile**

For the ten flight series the overall functional precision (RMSD) for the time paired relative humidity measurements was 3.75 %. The mean of the differences was 0.70 %. A mean difference of this size would normally indicate a bias, however in this case it is believed to be a simple artifact of the large variability in sensor data and the relatively small sample size. Table 3 is the summary statistics for the flight series.

| Time Paired Humidity Difference Statistics | | | | | |
|---|---|---|---|---|---|
| Intervals (hPa) | N Sample | Min | Max | Mean | RMSD |
| 19.9 to 0 | 8773 | -4 | 6.4 | 0.36 | 2.21 |
| 49.9 to 20 | 10569 | -8.6 | 9.4 | 1.42 | 3.85 |
| 99.9 to 50 | 8541 | -12.4 | 7.6 | 1.18 | 5.28 |
| 199.9 to 100 | 8747 | -13.9 | 6.7 | 0.68 | 3.99 |
| 299.9 to 200 | 4675 | -5 | 7.9 | 0.69 | 2.86 |
| 499.9 to 300 | 6537 | -10.9 | 9.3 | 0.51 | 3.39 |
| 849.9 to 500 | 7934 | -14.5 | 12.6 | -0.03 | 4.07 |
| 1070 to 850 | 3018 | -5.9 | 4.8 | 0.25 | 1.42 |
| ALL | 58794 | -14.5 | 12.6 | 0.70 | 3.75 |
| 400 to 4 | 44881 | -13.9 | 9.4 | 0.87 | 3.83 |
| SFC to 400 | 13913 | -14.5 | 12.6 | 0.17 | 3.51 |

**Table 3. Summary statistics for the time paired relative humidity differences.**

### 4.4 Statistical Analysis of u Wind Component Data.

For the entire flight series, 99% of the absolute u wind component differences for the time paired data were equal to or less than 0.8 m/s and 95% were equal to or less than 0.2 m/s. Figure 13 depicts the cumulative percentages for the absolute value of the u wind component differences, and figure 14 illustrates the distribution or the actual u wind component differences.

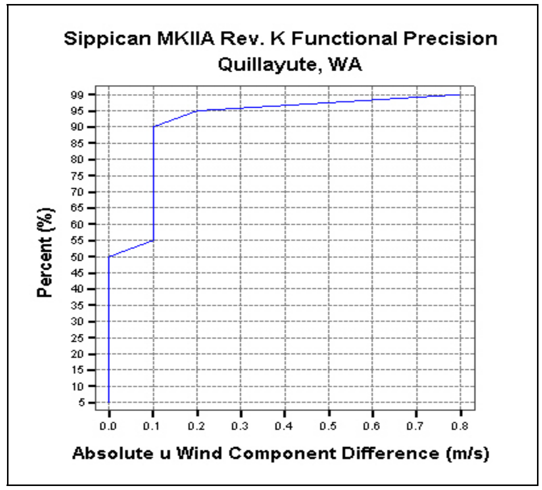


**Figure 13. Cumulative percentages of absolute u wind component differences.**

The y axis in figure 13 was scaled to 99 percent to maintain usefulness; large difference outliers in the last one percent compressed the x axis and reduced usefulness. The step appearance in the data is the result of the scale and data resolution. The interval size used for the histogram in figure 14 was 0.2 m/s.

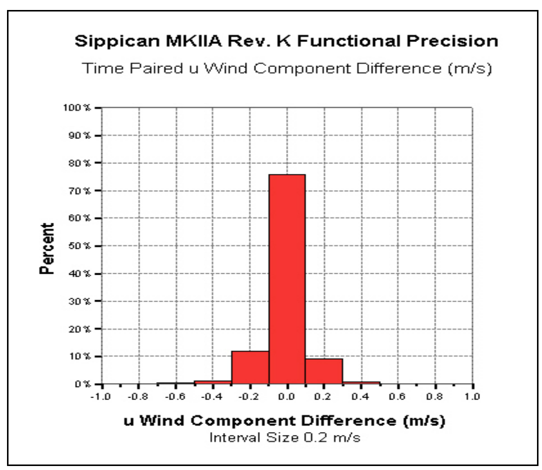


**Figure 14. Histogram of u wind component difference.**

The scatter plot shown in figure 15 indicates a number of outliers. Point B illustrates the effect of marginal GPS performance on one radiosonde. The outliers at points A are the result of missing data. These outliers are an artifact of one or both systems interpolating winds for the process data set. During this test there were no missing data attributed to radiosonde problems; in this case, the missing data was the result of outside influences.

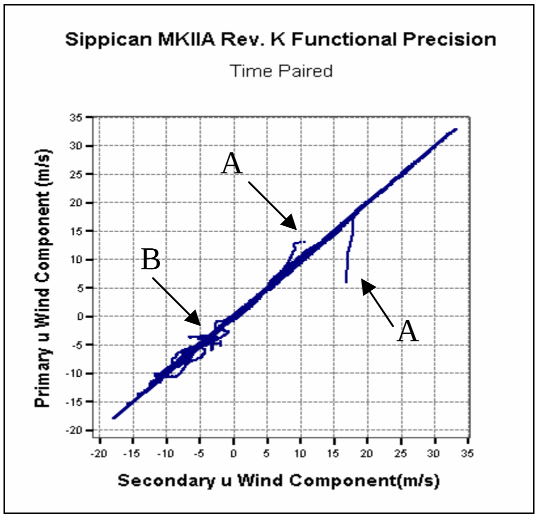


**Figure 15. Scatter plot of u wind component values for all flights.**

Figure 16a is a difference plot for the u Wind Components. In this case, the outliers illustrate the impact of the degradation in GPS that occurred on one of the two radiosondes flown. Whereas figure 16b depicts the typical GPS performance seen with this system, which is about 0.25 m/s difference between two identical instruments.

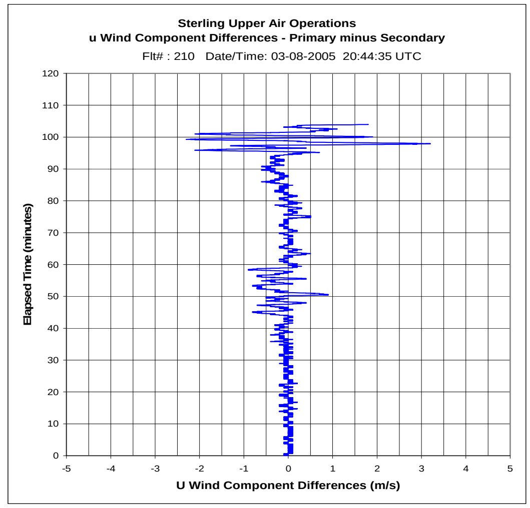


**Figure 16a. u Wind Component Difference**

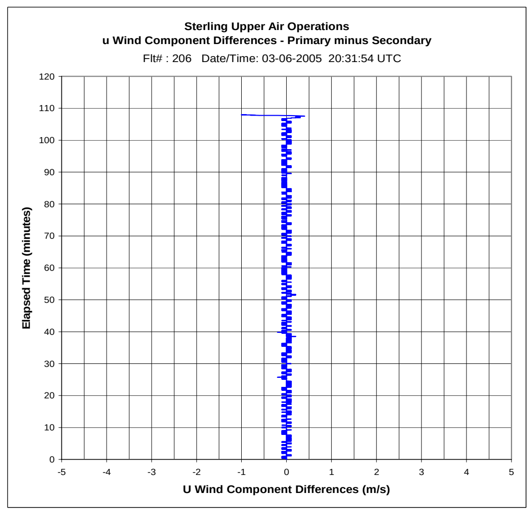


**Figure 16b. u Wind Component Difference**

For the ten flight series the overall functional precision (RMSD) for the time paired u wind component measurements was 0.27 m/s. The mean of the differences was 0.00 m/s. Table 4 is the summary statistics for the flight series.

| Time Paired u Wind Component Difference Statistics | | | | | |
|---|---|---|---|---|---|
| Intervals (hPa) | N Sample | Min | Max | Mean | RMSD |
| 19.9 to 0 | 8765 | -2.3 | 3.2 | 0.01 | 0.34 |
| 49.9 to 20 | 10382 | -0.7 | 1.3 | 0.02 | 0.13 |
| 99.9 to 50 | 7624 | -3.2 | 3.8 | -0.01 | 0.32 |
| 199.9 to 100 | 7870 | -10.7 | 0.9 | -0.05 | 0.48 |
| 299.9 to 200 | 4273 | -0.4 | 0.2 | -0.01 | 0.07 |
| 499.9 to 300 | 6001 | -0.2 | 0.2 | -0.01 | 0.06 |
| 849.9 to 500 | 7284 | -0.2 | 0.2 | 0.01 | 0.06 |
| 1070 to 850 | 2848 | -2.6 | 1.3 | -0.01 | 0.20 |
| ALL | 55047 | -10.7 | 3.8 | 0.00 | 0.27 |
| 400 to 4 | 42183 | -10.7 | 3.8 | -0.01 | 0.30 |
| SFC to 400 | 12765 | -0.2 | 0.2 | 0.00 | 0.06 |

**Table 4. Summary statistics for the time paired u wind component differences.**

### 4.5 Statistical Analysis of v Wind Component Data.

For the entire flight series, 99% of the absolute v wind component differences for the time paired data were equal to or less than 0.8 m/s, 95% of the differences were equal to or less than 0.2 m/s. Figure 17 shows the cumulative percentages for the absolute value of the v wind component differences, and figure 18 illustrates the distribution or the actual v wind component differences.

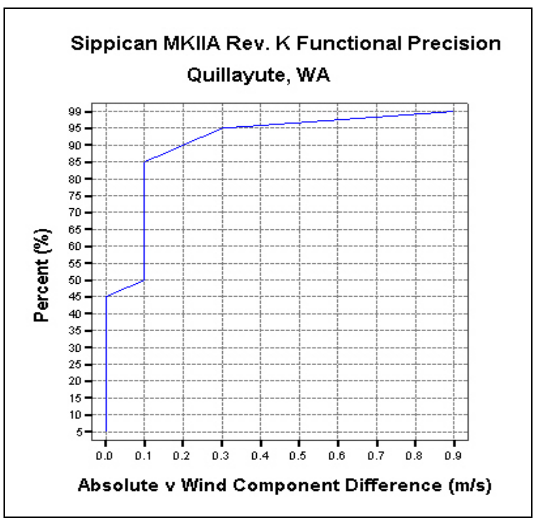


**Figure 17. Graph of cumulative percentages of absolute v wind component differences**

The y-axis in figure 17 was scaled to 99 percent to maintain usefulness; large difference outliers in the last one percent compressed the x-axis reduced usefulness. The step appearance in the data is the result of the scale and data resolution. For the histogram in figure 18 the interval size used for the bins was 0.2 m/s.

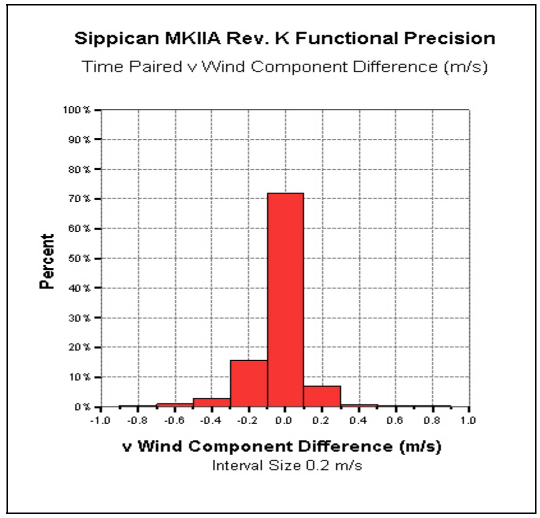


**Figure 18. Histogram of v wind component difference.**

The scatter plot shown in figure 19 indicates a number of outliers. These outliers are again attributed to the missing data discussed in section 4.4.

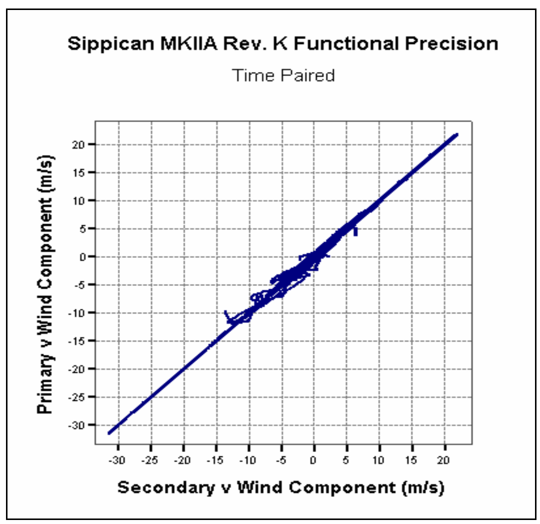


**Figure 19. Scatter plot of v wind component values for all flights.**

For the ten flight series the overall functional precision (RMSD) for the time paired v wind component measurements was 0.21 m/s. The mean of the differences was -0.01 m/s. Table 4 is the summary statistics for the flight series.

| Time Paired v Wind Component Difference Statistics | | | | | |
|---|---|---|---|---|---|
| Intervals (hPa) | N Sample | Min | Max | Mean | RMSD |
| 19.9 to 0 | 8765 | -2.3 | 3.9 | 0.00 | 0.34 |
| 49.9 to 20 | 10382 | -1.2 | 0.9 | -0.03 | 0.21 |
| 99.9 to 50 | 7624 | -2.7 | 2.1 | -0.03 | 0.28 |
| 199.9 to 100 | 7870 | -2.6 | 0.4 | -0.03 | 0.18 |
| 299.9 to 200 | 4273 | -0.2 | 0.2 | 0.00 | 0.08 |
| 499.9 to 300 | 6001 | -0.2 | 0.2 | 0.01 | 0.07 |
| 849.9 to 500 | 7284 | -0.2 | 0.4 | 0.01 | 0.07 |
| 1070 to 850 | 2848 | -2.5 | 2.1 | 0.00 | 0.20 |
| ALL | 55047 | -2.7 | 3.9 | -0.01 | 0.21 |
| 400 to 4 | 42183 | -2.7 | 3.9 | -0.02 | 0.24 |
| SFC to 400 | 12765 | -0.8 | 0.8 | 0.01 | 0.08 |

**Table 5. Summary statistics for the time paired v wind component differences.**

## 5. Conclusions

Although the results from this test are not conclusive due to the limited sample size, they do suggest some improvement has been made in the radiosondes functional precision. When this data set is contrasted against the MKIIA functional precision test of 2003, there is noted improvement in the thermodynamic data. For pressure, the Quillayute data set indicates marked improvement in performance over the 2003 data. The functional precision for Quillayute was 0.29 hPa and for the 2003 data set it was 0.54 hPa. For temperature, the Quillayute data set indicate minor improvement over the 2003 data. The functional precision was 0.26 ºC and for the 2003 data set was 0.31 ºC. It should be noted, that this test was conducted during a period when there was relatively low solar elevation angles. This may have minimized the amount of noise in the temperature data, which is suspected to exist during high solar elevation angles. For humidity, the Quillayute data set indicated moderate improvement over the 2003 data. The functional precision for Quillayute was 3.75 % and for the 2003 data set it was 4.27 %.

The GPS winds data were worse when compared to the 2003 data due to the reasons discussed in section 4.4. For the u and v wind components the functional precision for the Quillayute data were 0.27 m/s and 0.21 m/s respectively. The 2003 data set functional precision for u and v wind components were 0.12 m/s and 0.11 m/s respectively. This reduction in performance requires further investigation to eliminate any GPS data variability caused by ground equipment configuration.

It is important to emphasize that this report should be taken as merely an indication or first look at the radiosonde's performance due to the limited sample size. A more definitive answer of the functional precision of the RRS radiosonde will be forthcoming in another report.

## 6. References

World Meteorological Organization 1996: Guide to Meteorological Instruments and Methods of observation. Sixth Edition WMO-No. 8, Geneva.

NOAA Technical Report, NWS 44: Functional Precision of National Weather Service Upper-Air measurements Using VIZ Manufacturing Co. "A" Radiosonde (Model 1492-510)

ASTM Standard, E 177, Standard Practice for Use of the Terms Precision and Bias in Test Methods.

ASTM Standard, D 4430, Standard practice for Determining the Operational Comparability of Meteorological Measurements.

## 7. Acknowledgements

The authors of this paper wish to thank John Knox and Dick Pettipiece of the WFO Seattle, WA for coordinating and providing electronics support in preparation for the test. We also want to thank Linda McGivern, Michele Wishon, and Pat Scannell of the Quillayute upper air site for outstanding support during the test. Thanks to Paul Rockwood, Ivan R. Navarro, and Jefferey A. Paul for conducting all the Quillayute Functional Precision flights.